TiS Trends in Sciences
TRENDS IN SCIENCES 2027; 24(1): 14492
SPRINT Scholarly Publishing and Repository Integration Center
https://doi.org/10.48048/tis.2027.14492
RESEARCH ARTICLE

Phytochemical Profiling, Molecular Docking, and Biological Activities of *Psidium Guajava* and *Piper Betle* Extracts Incorporated into Chitosan-Based Hydrogel for Dental Wound Antimicrobial Applications

Parichat Thepthong[1,2], Panita Kongsune[1,2], Patcharakorn Raksasee[3], Safira Minham[3] and Netnapa Chana[2,4,*]

[1]*Department of Chemistry, Faculty of Science and Digital Innovation, Thaksin University, Phatthalung Campus, Phatthalung 93210, Thailand*
[2]*Innovative Material Chemistry for Environment Center, Department of Chemistry, Faculty of Science and Digital Innovation, Thaksin University, Phatthalung Campus, Phatthalung 93210, Thailand*
[3]*Paphayompittayakom School (SCiUS-Thaksin University), Phatthalung 93210, Thailand*
[4]*Department of Biotechnology, Faculty of Science and Digital Innovation, Thaksin University, Phatthalung Campus, Phatthalung 93210, Thailand*

([*]Corresponding author's e-mail: netnapa@tsu.ac.th)

Received: 23 May 2026, Revised: 6 July 2026, Accepted: 20 July 2026, Published: 10 September 2026

Abstract

Post-extraction dental wound management remains a clinical challenge owing to the risk of microbial infection and delayed tissue regeneration. This study evaluated water and ethanol extracts of four Thai medicinal plants, namely *Psidium guajava*, *Piper betle*, *Chromolaena odorata*, and *Tridax procumbens*, and developed chitosan/PVA hydrogels incorporating selected extracts. *P. betle* ethanol extract exhibited the highest total phenolic content (559.30 ± 15.25 mg GAE/g) and strongest DPPH radical scavenging activity (IC_{50} 14.46 ± 0.02 µg/mL), while *P. guajava* water and ethanol extracts demonstrated comparable antioxidant activity (IC_{50} 15.59 and 15.04 µg/mL, respectively). *P. guajava* water, *P. guajava* ethanol, and *P. betle* ethanol extracts were incorporated into chitosan/PVA hydrogels. The *P. guajava* water extract formulation produced the largest inhibition zones against *S. mutans* (13.86 ± 0.09 mm), *S. aureus* (13.58 ± 0.08 mm), and *E. coli* (17.44 ± 0.13 mm). Release profiling revealed distinct patterns: The *P. guajava* water extract hydrogel achieved peak phenolic release (2.38 mg GAE/mL) at 6 h, while the *P. betle* ethanol extract hydrogel showed prolonged release up to 24 h (1.60 mg GAE/mL). LC-MS/MS profiling annotated 24 compounds in *P. guajava* water extract, predominantly flavonoids and phenolic acids. Molecular docking against COX-2 predicted that myricetin and quercetin exhibited favorable binding free energies of -8.68 and -8.59 kcal/mol, surpassing that of ibuprofen (-6.77 kcal/mol), with interactions at key active site residues including SER530, SER354, TYR356, GLN193, MET523, and HIS90. Collectively, these *in vitro* findings provide preliminary evidence supporting the potential of *P. guajava* water extract-loaded chitosan/PVA hydrogel as a plant-derived biomaterial candidate for post-extraction dental wound management.

Keywords: *Psidium guajava*, *Piper betle*, Chitosan hydrogel, Antimicrobial activity, Molecular docking, Dental application

Introduction

Dental extraction ranks among the most frequently performed oral surgical procedures worldwide, yet post-extraction complications such as alveolar infection, localized inflammation, and impaired wound healing continue to pose significant clinical challenges. A recent narrative review reported that otherwise healthy patients undergoing third molar extraction face approximately a 10% risk of post-operative infection. This rate increases to 25% in immunocompromised individuals,

underscoring the need for more effective post-extraction wound management strategies. Traditional wound management strategies, including systemic antibiotic therapy, chemical antiseptics, and physical debridement, offer limited capacity for sustained infection control and do not actively promote tissue regeneration [1]. Moreover, conventional antimicrobial agents are increasingly limited by antimicrobial resistance, poor biofilm penetration, and adverse mucosal effects. The rise of drug-resistant bacterial pathogens highlights the urgent need for novel antimicrobial strategies that deliver effective, long-lasting treatment directly at the wound site with minimal side effects [2].

Hydrogels have emerged as highly promising biomaterials for wound care applications owing to their high-water content, biocompatibility, and capacity to sustain a moist healing environment conducive to tissue regeneration. Among these, chitosan-based hydrogels have garnered significant interest due to their intrinsic antimicrobial activity, biodegradability, mucoadhesive properties, and demonstrated ability to accelerate wound closure [3-5]. Recent studies have further validated that chitosan hydrogels enriched with natural plant extracts can synergistically enhance infection control and tissue regeneration, offering a multifunctional platform for advanced wound dressing applications. The integration of bioactive plant extracts into such polymeric matrices therefore represents a viable strategy for developing next-generation dental wound dressings [6].

Several tropical medicinal plants have been investigated for their potential in oral wound care applications, including *Chromolaena odorata*, *Piper betle*, *Psidium guajava*, and *Tridax procumbens*. These plants possess well-documented antimicrobial, anti-inflammatory, and wound-healing properties [7-10]. Among these, *P. guajava* and *P. betle* are widely recognized medicinal plants with well-documented pharmacological profiles. *P. guajava* leaf extract is rich in bioactive phenolic compounds and flavonoids, including gallic acid, quercetin, and catechin, which exhibit potent antimicrobial activity through multiple mechanisms, including disruption of bacterial cell membranes, inhibition of essential enzymes, and interference with quorum sensing mechanisms that regulate biofilm formation [11,12]. Notably, these bioactive constituents have been reported to effectively inhibit oral bacteria, particularly *Streptococcus mutans*, by suppressing biofilm formation, reducing bacterial adhesion, and inhibiting acid production responsible for dental caries [10]. Both *P. betle* and *P. guajava* extracts have been shown to exert bacteriostatic effects on early dental plaque bacteria by creating a stressed microenvironment that suppresses bacterial growth and propagation, suggesting their particular relevance to oral health applications [13,14]. Beyond antimicrobial activity, the primary bioactive constituents of *P. guajava* leaves, including gallic acid, quercetin, catechin, and chlorogenic acid, have demonstrated potent antioxidant effects through scavenging of reactive oxygen species (ROS) and enhancement of endogenous antioxidant enzymes such as superoxide dismutase (SOD) and catalase, as well as antioxidant molecules such as glutathione. These compounds also exert anti-inflammatory effects through suppression of pro-inflammatory cytokines (TNF-α, IL-6, and IL-1β) and inhibition of inflammatory enzymes cyclooxygenase-2 (COX-2) and iNOS via the NF-κB and MAPK signaling pathways [10,15].

Despite growing evidence of their individual bioactivities, the systematic development and characterization of chitosan hydrogels loaded with *P. guajava* and *P. betle* extracts for dental wound applications remains largely unexplored. Waresindo *et al*. [16] developed a polyvinyl alcohol (PVA) hydrogel incorporated with *P. guajava* leaf extract using a freeze-thaw method. The resulting hydrogel demonstrated exudate absorption capacity and antibacterial activity, in which the extract served as an antimicrobial agent while PVA provided a biocompatible and non-toxic matrix. These findings suggest its promising potential for wound care applications in the biomedical industry. However, chitosan/PVA composite hydrogels offer distinct advantages for wound dressing applications, combining the inherent antimicrobial properties, superior biocompatibility, biodegradability, and mucoadhesive characteristics of chitosan with the hydrophilicity and film-forming ability of PVA, making them particularly favorable for intraoral wound environments [17,18]. The incorporation of plant-derived bioactive extracts into such composite matrices may therefore produce a synergistic effect that enhances both antimicrobial and wound healing efficacy while reducing reliance on synthetic antimicrobial agents. This is of particular clinical relevance given the

increasing concern over antimicrobial resistance and the growing demand for natural, biocompatible alternatives in dental therapeutics. This study therefore aims to evaluate the antioxidant and antimicrobial properties of water and ethanol extracts from tropical medicinal plants, to develop and characterize extract-loaded chitosan hydrogels and assess their phenolic compound release profile, to identify key bioactive compounds, and to investigate the molecular interactions of identified flavonoids with COX-2 via molecular docking as a mechanistic basis for potential anti-inflammatory activity. The findings of this study are anticipated to provide a scientific basis for the development of plant-derived chitosan hydrogels as effective and safe biomaterials for post-dental extraction wound care.

Materials and methods

Materials

Fresh leaves of *Chromolaena odorata*, *Piper betle*, *Psidium guajava*, and *Tridax procumbens* were collected from Phatthalung province, Thailand. Plant identification was confirmed based on their distinctive morphological characteristics by Dr. Paweena Kaewubon, a botanist at Thaksin University. Collected leaves were washed under running tap water and dried in a hot-air oven at 50 °C until the moisture content reached below 5%. Dried leaves were ground into fine powder using an electric blender and sieved through a 40-mesh screen. Plant powder (10 g) was subjected to ultrasound-assisted extraction (UAE) at 40 kHz and 150 W for 30 min at 40 °C, with a solid-to-solvent ratio of 1:10 (w/v). Two solvents were employed independently: 95% ethanol and deionized water. Ethanol extracts were filtered through Whatman No. 1 filter paper and concentrated under reduced pressure using a rotary evaporator (Büchi R-300, Switzerland) at 45 °C, while aqueous extracts were lyophilized using a freeze dryer (Christ Delta 2-24 LSCplus, Martin Christ, Germany) at a condenser temperature of -55 °C. All crude extracts were stored at 4 °C in amber vials until use. Extraction yield was expressed as percentage of dried extract weight relative to the initial plant powder weight (%, w/w).

Chemicals

Chitosan (50,000 - 190,000 Da with ≥ 75% degree of deacetylation), polyvinyl alcohol (PVA, 99% hydrolyzed), 2,2-diphenyl-1-picrylhydrazyl (DPPH), Folin-Ciocalteu reagent, gallic acid, chlorhexidine gluconate, dimethyl sulfoxide (DMSO), and ascorbic acid were purchased from Sigma-Aldrich (St. Louis, MO, USA). Mueller-Hinton agar, Mueller-Hinton broth, Brain Heart Infusion (BHI) agar, BHI broth, and blood agar base were obtained from Thermo Fisher Scientific. Blood agar plates were prepared by supplementing blood agar base with 5% defibrinated sheep blood prior to use. Phosphate buffered saline (PBS, pH 6.8) was prepared in-house according to standard procedures. All chemicals were of analytical grade.

Biological activities evaluation

Total phenolic content (TPC)

Total phenolic content (TPC) was determined using the Folin-Ciocalteu colorimetric method. Briefly, 0.06 mL of extract solution (1 mg/mL) was mixed with 2.5 mL of Folin-Ciocalteu reagent (diluted 10-fold with distilled water) and allowed to react for 5 min at room temperature in the dark. Subsequently, 2 mL of sodium carbonate solution (7.5%, w/v) was added and the mixture was incubated for 15 min at 50 °C. Absorbance was measured at 765 nm using a UV-Vis spectrophotometer. TPC was calculated from a gallic acid standard calibration curve and expressed as milligrams of gallic acid equivalent per gram of dry extract (mg GAE/g dry extract). All measurements were performed in triplicate.

DPPH radical scavenging activity

Antioxidant capacity was assessed using the DPPH free radical scavenging assay following the method of Kongsune *et al.* [19] with slight modifications. Extract solutions at various concentrations were prepared in their respective extraction solvents (95% ethanol or deionized water). An aliquot of 100 µL of each concentration was mixed with 2.9 mL of 0.1 mM DPPH solution in methanol and incubated for 30 min at room temperature in the dark. Absorbance was recorded at 517 nm using a UV-Vis spectrophotometer, with ascorbic acid as a positive control. The percentage of DPPH radical scavenging activity was calculated as follows.

$$\% \text{ inhibition} = \frac{A_{control} - A_{sample}}{A_{control}} \times 100 \quad (1)$$

where $A_{control}$ is the absorbance of control (respective solvent with DPPH solution) and A_{sample} is the absorbance of sample. The half-maximal inhibitory concentration (IC_{50}) was determined from the dose-response curve by linear regression analysis. All measurements were performed in triplicate.

Antimicrobial activity

Antibacterial activity was assessed using the agar well diffusion method against three clinically relevant microorganisms, namely *Streptococcus mutans* ATCC 25175, *Staphylococcus aureus* ATCC 25923, and *Escherichia coli* ATCC 25922. For *S. aureus* and *E. coli*, bacterial suspensions were prepared at 0.5 McFarland standard turbidity (approximately 1.5×10^8 CFU/mL) and uniformly spread onto Mueller-Hinton agar (MHA) plates. For *S. mutans*, bacterial suspension at the same turbidity was inoculated into Brain Heart Infusion (BHI) agar at approximately 50 °C, mixed homogeneously, and poured onto plates containing 6 mm diameter steel rods. After solidification, the rods were removed to create uniform wells.

For all plates, 50 µL of each extract (5 mg/mL in 10% DMSO) was loaded into each well. Chlorhexidine gluconate (1.2 mg/mL) served as positive controls for *S. mutans*, while 10% DMSO served as the negative control and was previously confirmed to exhibit no inhibitory effect on the tested microorganisms. MHA plates were incubated aerobically at 37 °C for 24 h, while BHI plates containing *S. mutans* were incubated under anaerobic conditions at 37 °C for 18 - 24 h. Inhibition zone diameters, including the well diameter (6 mm), were measured in millimeters using a digital caliper. All assays were performed in triplicate.

Given that *S. mutans* is the primary etiological agent of dental caries and a key contributor to post-extraction wound contamination, minimum inhibitory concentration (MIC) and minimum bactericidal concentration (MBC) determination was prioritized for this organism as the most clinically relevant target for the intended dental wound application. MIC and MBC were determined using the broth microdilution method. Serial two-fold dilutions of each extract were prepared in BHI broth in a round-bottomed 96-well polystyrene microtiter plate, with a final volume of 200 µL per well. Bacterial suspension (1.5×10^8 CFU/mL) was added at 100 µL per well. Plates were incubated under anaerobic conditions at 37 °C for 24 h. The MIC was defined as the lowest concentration at which no visible turbidity was observed. To determine the MBC, 10 µL from each clear well was subcultured onto Blood agar (BA) plates and incubated at 37 °C for 24 h. The MBC was defined as the lowest concentration at which no colony growth was observed. All assays were performed in triplicate.

LC-MS/MS chemical profiling

Phytochemical profiling of *P. guajava* leave water extracts was performed using liquid chromatography coupled with tandem mass spectrometry (LC-MS/MS) on an Agilent 1290 Infinity II UHPLC system coupled to an Agilent 6545 Quadrupole Time-of-Flight (QTOF) mass spectrometer (Agilent Technologies, USA). Prior to analysis, the extract (10 mg) was dissolved in 1 mL of LC-grade ethanol, sonicated for 30 min, centrifuged at 10,000 rpm at 4 °C for 5 min, and filtered through a 0.22 µm nylon membrane filter before injection. Chromatographic separation was achieved on a Zorbax Eclipse Plus C18 Rapid Resolution HD column (2.1×100 mm, 1.8 µm particle size; Agilent Technologies, USA) with a guard column (Zorbax Eclipse Plus C18, 2.1×5 mm, 1.8 µm), maintained at 40 °C. The mobile phase consisted of 0.1% (v/v) formic acid in water (solvent A) and 0.1% (v/v) formic acid in 80% acetonitrile/20% water (solvent B), delivered at a flow rate of 0.2 mL/min using the following gradient elution program: 0 - 45 min, 0% - 100% B; 45 - 50 min, 100% B; 50 - 60 min, 100% - 0% B; 60 - 65 min, 0% B. The injection volume was 2 µL and the total run time was 65 min. Mass spectrometric detection was performed in negative ionization mode (ESI^-) using a Dual Agilent Jet Stream (AJS) ion source with the following parameters: Gas temperature 325 °C, drying gas flow 13 L/min, nebulizer pressure 35 psig, sheath gas temperature 275 °C, sheath gas flow 12 L/min, capillary voltage 4,000 V, nozzle voltage 2,000 V, and fragmentor voltage 175 V. Data were acquired in AutoMSMS mode with an MS scan range of m/z 100 - 1,200 and an MS/MS scan range of m/z 50 - 1,200, using fixed collision energies of 10, 20, and 40 V. Mass accuracy was maintained using internal reference masses at m/z 112.9856 (deprotonated trifluoroacetic

acid) and m/z 1033.9881 (TFA-adducted HP-921) in negative ion mode. Data analysis was performed using Agilent MassHunter Qualitative Analysis Workflows software (Version B.08.00, Service Pack 1). Compound identification was performed by comparing observed accurate masses and MS/MS fragmentation patterns with the METLIN Personal Compound Database (PCD) and Personal Compound Database and Library (PCDL), Version 8. The library match score represents the percentage match between experimental and reference mass spectra. Compounds with a library match score of ≥ 80 were tentatively identified based on accurate mass, MS/MS fragmentation patterns, and Metlin library matching. Compounds with scores below 80 were considered putative annotations based on partial library matching, while those with no available library match (score = 0) were putatively annotated based on accurate mass data alone.

Molecular docking

Molecular docking analysis was performed to investigate the binding interactions of myricetin and quercetin, identified by LC-MS/MS analysis, with cyclooxygenase-2 (COX-2), using AutoDock 4.2 software (The Scripps Research Institute, La Jolla, CA, USA). The three-dimensional crystal structure of COX-2 (PDB ID: 4PH9, resolution 1.81 Å) was retrieved from the RCSB Protein Data Bank (https://www.rcsb.org). Protein preparation was performed using AutoDockTools 1.5.7, including the removal of water molecules, heteroatoms, and co-crystallized ligands, addition of polar hydrogen atoms, and assignment of Kollman partial charges. The three-dimensional structures of myricetin, quercetin, ibuprofen, and celecoxib were constructed using GaussView 5.0.8 and geometry-optimized at the HF/6-31G basis set using the Gaussian09 program. Gasteiger partial charges were assigned and rotatable bonds were defined for each ligand prior to docking. To validate the docking protocol, ibuprofen, the co-crystallized ligand of the selected crystal structure (PDB ID: 4PH9) [20], was redocked into the prepared COX-2 structure, and the reproduced binding pose was evaluated against the original X-ray crystallographic conformation to confirm the reliability of the docking setup. A grid box of 84×84×84 grid points with a spacing of 0.375 Å was centered on the active site of COX-2, defined based on the position of the co-crystallized ligand. Conformational searching was performed using the Lamarckian genetic algorithm (LGA) with 100 independent docking runs per ligand. Docking results were clustered using an RMSD threshold of 2.0 Å, and the binding pose with the lowest free energy of binding (kcal/mol) within the most populated cluster was selected as the most favorable binding conformation. Ibuprofen and celecoxib were retained as reference ligands representing a non-selective NSAID and a selective COX-2 inhibitor, respectively, for comparative binding affinity assessment against the test flavonoids.

Hydrogel preparation and characterization

Hydrogel preparation

Chitosan was dissolved in 1% (w/v) acetic acid solution under constant stirring until a clear homogeneous solution was obtained. Polyvinyl alcohol (PVA, 99% hydrolyzed) was dissolved separately in deionized water at 90 °C. The two polymer solutions were combined at five chitosan: PVA weight ratios (2:0, 1.75:0.25, 1.50:0.50, 1.25:0.75, and 1:1, w/w) and stirred continuously on a hotplate stirrer at 50 °C until homogeneous. Glycerin was subsequently added at 20% (w/w) relative to total polymer weight as a plasticizer to improve mechanical flexibility, followed by the addition of a trisodium citrate at 2% (w/w) of total polymer weight to enhance hydrogel network stability. Selected plant extracts were incorporated into the polymer mixture at a final concentration of 5 mg/mL and blended thoroughly before casting into standardized molds. Structural interactions between hydrogel components and incorporated plant extracts were confirmed by Fourier transform infrared (FTIR) spectroscopy (Perkin Elmer, USA) in attenuated total reflectance (ATR) mode, scanning over the wavenumber range of 4,000 - 400 cm^{-1} at a spectral resolution of 4 cm^{-1} with 32 accumulated scans.

Swelling behavior

The swelling behavior of hydrogel formulations was assessed by immersing pre-weighed hydrogel discs (diameter 10 mm, approximately 0.5 g) in PBS solution at 37 °C and recording weight changes at 30, 60, and 90 min. At each time point, swollen hydrogels were carefully removed and gently blotted with filter paper to eliminate surface water before immediate weighing.

Percentage swelling was calculated according to the following equation.

$$\% \text{ Swelling} = [\frac{W_{swollen} - W_{dry}}{W_{dry}}] \times 100 \quad (2)$$

where $W_{swollen}$ and W_{dry} denote the weight of the swollen and dry hydrogel, respectively. All measurements were performed in triplicate.

Biological evaluation of hydrogel formulations

Antibacterial activity of the extract-loaded hydrogel formulations was assessed against *S. mutans*, *S. aureus*, and *E. coli* using the agar well diffusion method as described above. Hydrogel samples (approximately 0.1 g) were loaded into 6 mm wells punched into the solidified agar. Chlorhexidine gluconate (0.12%, w/v) and the plain chitosan/PVA hydrogel without extract served as positive and negative controls, respectively. Inhibition zone diameters were measured in millimeters using a digital caliper. All assays were performed in triplicate.

Phenolic compound release profiles were evaluated by immersing hydrogel discs (diameter 10 mm, approximately 0.5 g) in 5 mL of PBS (pH 6.8) at 37 °C with gentle agitation at 50 rpm to simulate oral physiological conditions. Aliquots of 200 µL were withdrawn at 6 and 24 h and immediately replaced with equal volumes of fresh PBS to maintain sink conditions throughout the experiment. Cumulative phenolic release was calculated by accounting for the volume replacement at each sampling point. Total phenolic content of collected fractions was determined using the Folin-Ciocalteu method and expressed as milligrams of gallic acid equivalent per milliliter of release medium (mg GAE/mL). Antioxidant activity of the release fractions was determined by DPPH radical scavenging assay and expressed as percentage inhibition (% inhibition) at the concentration present in each collected fraction, as described above. All measurements were performed in triplicate.

Statistical analysis

All experiments were performed in triplicate, and results were expressed as mean ± standard deviation (SD). Statistical analysis was performed using one-way analysis of variance (ANOVA) followed by Duncan's multiple range test for post-hoc comparison using SPSS Statistics software. A p-value of less than 0.05 was considered statistically significant.

Results and discussion

Antioxidant activity and total phenolic content of plant extracts

The antioxidant activity and total phenolic content (TPC) of water and ethanol extracts from four Thai medicinal plants varied significantly across species and extraction solvents (**Table 1**). For most species, ethanol extracts demonstrated superior DPPH radical scavenging activity compared to their water counterparts, a trend consistent with the higher solubility of polyphenolic compounds in polar organic solvents [21]. However, *P. guajava* represented a notable exception, in which the water extract yielded a TPC approximately 1.3-fold higher than its ethanol counterpart (303.65 vs. 229.06 mg GAE/g extract), while DPPH radical scavenging activity was not significantly different between the two solvents. This suggests that certain polar phenolic compounds in *P. guajava* leaves, possibly including quinic acid, gallic acid, and catechin glycosides, are more efficiently extracted by aqueous media.

Among all tested extracts, *P. betle* ethanol extract exhibited the highest TPC (559.30 ± 15.25 mg GAE/g dry extract) and the strongest DPPH radical scavenging activity, with 87.69 ± 0.35% inhibition at 160 µg/mL and an IC_{50} of 14.46 ± 0.02 µg/mL. This was followed by *P. guajava* water extract (TPC = 303.65 ± 12.48 mg GAE/g dry extract; IC_{50} = 15.59 ± 0.02 µg/mL) and *P. guajava* ethanol extract (TPC = 229.06 ± 10.35 mg GAE/g dry extract; IC_{50} = 15.04 ± 0.03 µg/mL). The exceptionally high TPC of *P. betle* ethanol extract is attributed to its rich content of hydroxychavicol, eugenol, and allylpyrocatechol, phenolic compounds well-documented as primary contributors to the strong antioxidant capacity of betel leaf. The high TPC observed in the present study (559.30 ± 15.25 mg GAE/g dry extract) considerably exceeds values reported in previous studies on *P. betle* leaf extracts, including 261.904 mg GAE/g dry extract from ultrasound-assisted extraction, and 260.3 mg GAE/g dry extract from ethanolic maceration [22,23]. This may be attributed to differences in plant variety, geographical origin, drying conditions, and the use of 95% ethanol,

which effectively solubilizes hydrophobic phenolic constituents such as hydroxychavicol and eugenol that are characteristic of *P. betle* leaves [23].

Both *P. guajava* water and ethanol extracts demonstrated comparable DPPH inhibition, with IC_{50} values of 15.59 ± 0.02 and 15.04 ± 0.03 µg/mL, respectively, indicating strong antioxidant activity. These IC_{50} values were approximately 1.8-fold higher than the IC_{50} of 8.33 µg/mL reported by Dehideniya *et al*. [24], indicating comparatively lower antioxidant activity, which may be attributed to differences in extraction technique and process intensity. Nevertheless, the results of the present study remain within a comparable range and confirm the substantial antioxidant potential of guava leaf extracts. Notably, the *P. guajava* water extract yielded a TPC approximately 1.3-fold higher than its ethanol counterpart (303.65 vs. 229.06 mg GAE/g dry extract), suggesting that certain polar phenolic compounds, possibly including quinic acid, gallic acid, and catechin glycosides, are more efficiently solubilized in aqueous media. Seo *et al*. [25] demonstrated that the relationship between solvent polarity and phenolic extraction from guava leaves is complex, with water extracting higher amounts of certain phenolic classes while hydroethanolic mixtures optimize overall antioxidant capacity.

In contrast, *C. odorata* and *T. procumbens* extracts demonstrated considerably lower antioxidant activity, with DPPH inhibition values below 23% at the highest tested concentration of 160 µg/mL. *T. procumbens* ethanol extract recorded the lowest TPC of all samples (3.44 ± 0.53 mg GAE/g dry extract), which may explain its weak DPPH radical scavenging capacity. Notably, the *C. odorata* water extract displayed a comparatively high TPC value (98.64 ± 2.64 mg GAE/g dry extract) despite exhibiting minimal DPPH inhibition (9.10 ± 0.53%). This discrepancy may be attributed to non-specific reactivity of the Folin-Ciocalteu reagent with reducing substances beyond phenolic compounds, such as reducing sugars and ascorbic acid, which can lead to TPC overestimation in complex crude plant extracts [26,27]. These findings suggest that these two species are less suitable candidates for antioxidant-based dental wound dressing applications, particularly when compared to the strong activity observed for *P. betle* and *P. guajava*. However, the reference antioxidant ascorbic acid showed a considerably lower IC_{50} (3.12 ± 0.01 µg/mL), reflecting its well-characterized hydrogen atom transfer mechanism and high molar reactivity toward DPPH radicals, compared to the more complex multicomponent action of crude plant extracts. The IC_{50} values for *P. betle* and *P. guajava* extracts, while higher than ascorbic acid, are still considered within the range of strong antioxidant activity and are particularly promising in the context of dental wound management, where sustained oxidative stress from inflammatory mediators represents a key barrier to healing. Based on these results, *P. guajava* water and ethanol extracts and *P. betle* ethanol extract were selected for further biological characterization and hydrogel development owing to their superior antioxidant capacity, measurable IC_{50} values, and high TPC.

Table 1 Antioxidant activity and total phenolic content of water and ethanol extracts from Thai medicinal plants. Values are presented as mean ± SD (*n*=3).

Scientific names	Solvents	% Yields	Total phenolic content (mg GAE/g dry extract)	DPPH inhibition	
				%	IC_{50}; µg/mL
Chromolaena odorata	water	21.67 ± 2.36^{a}	98.64 ± 2.64^{d}	9.10 ± 0.53^{d}	ND
	95% ethanol	7.22 ± 0.96^{c}	115.14 ± 4.58^{d}	22.52 ± 0.40^{c}	ND
Tridax procumbens	water	11.50 ± 0.00^{b}	24.14 ± 0.33^{f}	2.04 ± 0.23^{e}	ND
	95% ethanol	5.96 ± 3.12^{d}	3.44 ± 0.53^{g}	6.39 ± 3.27^{d}	ND
Piper betle	water	14.00 ± 1.80^{b}	71.39 ± 2.21^{e}	37.59 ± 1.18^{b}	ND
	95% ethanol	9.52 ± 0.24^{c}	559.30 ± 15.25^{a}	87.69 ± 0.35^{a}	14.46 ± 0.02^{b}

Scientific names	Solvents	% Yields	Total phenolic content (mg GAE/g dry extract)	DPPH inhibition	
				%	IC_{50}; µg/mL
Psidium guajava	water	11.83 ± 0.58[b]	303.65 ± 12.48[b]	87.62 ± 0.66[a]	15.59 ± 0.02[b]
	95% ethanol	12.41 ± 2.48[b]	229.06 ± 10.35[c]	88.59 ± 0.08[a]	15.04 ± 0.03[b]
Ascorbic acid	-	-	-	ND	3.12 ± 0.01[a]

Note: DPPH = 2,2-diphenyl-1-picrylhydrazyl; IC_{50} = concentration required for 50% inhibition; mg GAE/g = milligrams of gallic acid equivalent per gram of extract; ND = Not Determined (inhibition below 50% at the highest tested concentration). Different letters within the same column indicate significant differences ($p < 0.05$). Percentage DPPH inhibition measured at 160 µg/mL extract concentration.

Antibacterial activity of plant extracts

Oral pathogens including *Streptococcus mutan*s, *Staphylococcus aureus*, and *Escherichia coli* play central roles in the pathogenesis of dental infection and post-extraction wound complications. *S. mutans* is the primary cariogenic bacterium responsible for biofilm-mediated acid production and enamel demineralization, while *S. aureus* and *E. coli* are opportunistic pathogens commonly implicated in secondary oral wound infections and periapical abscess formation [28]. In the present study, the antibacterial activity of all eight plant extracts was evaluated against three clinically relevant bacteria using the agar well diffusion method, and results are presented in **Figure 1** and **Table 2**. All extracts demonstrated inhibitory activity against *Streptococcus mutans*, with inhibition zones ranging from 8.3 to 14.2 mm. The *P. guajava* water extract produced the largest inhibition zone (14.2 ± 0.40 mm), followed by *P. guajava* ethanol extract (11.7 ± 0.50 mm) and *P. betle* water extract (11 ± 0.01 mm), with statistically significant differences from the remaining extracts ($p < 0.05$). The strong activity against *S. mutans* is clinically relevant, as this bacterium is the primary etiological agent of dental caries and a key contributor to post-extraction wound contamination. The MIC of *P. guajava* water and ethanol extracts against *S. mutans* was 1.25 mg/mL, with an MBC of 2.5 mg/mL. In contrast, *T. procumbens*, *C. odorata*, and *P. betle* extracts did not achieve complete bactericidal activity at the highest tested concentration (2.5 mg/mL). The positive control chlorhexidine exhibited an MBC of 0.002 mg/mL.

Both *P. guajava* water and ethanol extracts additionally exhibited broad-spectrum activity against *S. aureus* and *E. coli*, with the water extract consistently producing larger inhibition zones (12.8 ± 0.40 and 14.3 ± 0.50 mm, respectively) than the ethanol extract (10.3 ± 0.50 and 11.3 ± 0.50 mm, respectively). Activity against *E. coli*, a Gram-negative species generally considered less susceptible due to its outer membrane lipopolysaccharide barrier, may reflect the high TPC of the water extract (303.65 ± 12.48 mg GAE/g dry extract) and synergistic interactions among phenolic constituents. The antimicrobial activity of *P. guajava* extract has been associated with its bioactive phenolic compounds, including quercetin, avicularin (quercetin-3-O-arabinoside), gossypetin, epicatechin, and ellagic acid, identified predominantly in the ethyl acetate and aqueous partitions, which exhibited inhibitory activity against foodborne pathogens including *Escherichia coli*, *Salmonella* Typhimurium, and *Staphylococcus aureus* [29].

The superior antibacterial activity of *P. guajava* extracts, despite their lower TPC compared to *P. betle* ethanol extract, suggests that antibacterial efficacy is determined not solely by total phenolic content, but by the specific composition and synergistic interactions of bioactive compounds present in the extract. Allylpyrocatechol, a principal phenolic derivative of *P. betle* closely related to hydroxychavicol, has been reported to exert antibacterial activity against oral pathogens through inhibition of MurA, a key enzyme catalyzing the first step of peptidoglycan biosynthesis in bacterial cell wall formation [30]. Nevertheless, the inhibition zones produced by *P. guajava* water extract against *S. mutans* are considered clinically meaningful and comparable to values reported for other plant-derived dental antimicrobial candidates. Notably, *P. guajava* water and ethanol extracts also demonstrated broad-spectrum activity against *S. aureus* and *E. coli*,

with inhibition zones of 12.8 ± 0.40 and 10.3 ± 0.50 mm against *S. aureus*, and 14.3 ± 0.50 and 11.3 ± 0.50 mm against *E. coli*, respectively. *C. odorata* and *T. procumbens* extracts demonstrated limited activity, restricted to 8.7 - 10 mm against *S. mutans*, consistent with their low TPC and weak antioxidant activity.

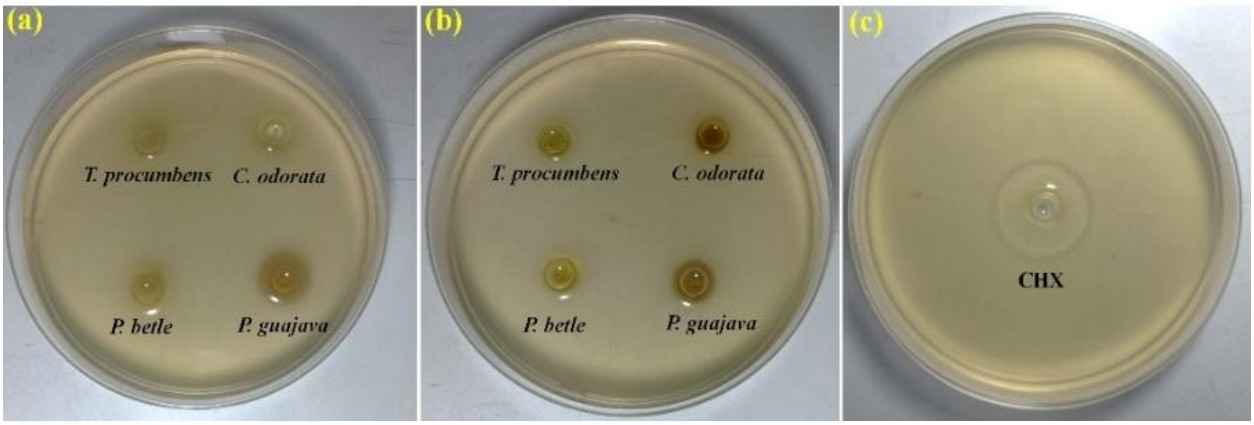


Figure 1 Inhibition zones of plant extracts against *Streptococcus mutans* using the agar well diffusion method. (a) Water extracts and (b) 95% ethanol extracts of *Tridax procumbens*, *Chromolaena odorata*, *Piper betle*, and *Psidium guajava* at a concentration of 5 mg/mL. (c) Chlorhexidine (CHX) at 1.2 mg/mL as a positive control.

Based on the comprehensive biological screening results, *P. guajava* water extract, *P. guajava* ethanol extract, and *P. betle* ethanol extract were selected for incorporation into chitosan-based hydrogels. *P. guajava* water extract was prioritized as the lead formulation owing to its broad-spectrum antibacterial activity and high TPC, while *P. betle* ethanol extract was retained for its superior antioxidant potential, which may complement wound healing through oxidative stress mitigation.

Table 2 Antibacterial activity of plant extracts against oral and pathogenic bacteria. Values are presented as mean ± SD (n=3).

Samples	Inhibition zone (mm)			MIC	MBC
	S. mutans	***S. aureus***	***E. coli***	***S. mutans***	***S. mutans***
*T. procumbens*_water	10 ± 0.00^{d}	NT	NT	> 1.25	> 2.5
*T. procumbens*_ethanol	9.7 ± 0.50^{d}	NT	NT	> 1.25	> 2.5
*C.odorata*_water	10 ± 0.00^{d}	NT	NT	> 1.25	> 2.5
*C.odorata*_ethanol	8.7 ± 0.50^{e}	NT	NT	> 1.25	> 2.5
*P. betle*_water	11 ± 0.01^{c}	NT	NT	> 1.25	> 2.5
*P. betle*_ethanol	8.3 ± 0.50^{e}	NT	NT	> 1.25	> 2.5
*P. guajava*_water	14.2 ± 0.40^{b}	12.8 ± 0.40^{a}	14.3 ± 0.50^{a}	1.25	2.5
*P. guajava*_ethanol	11.7 ± 0.50^{c}	10.3 ± 0.50^{b}	11.3 ± 0.50^{b}	1.25	2.5
Chlorhexidine (CHX)	25.8 ± 0.40^{a}	–	–	0.001	0.002

All plant extracts were tested at a concentration of 5 mg/mL; chlorhexidine (CHX) served as a positive control at 1.2 mg/mL. NT = Not tested. MIC: Lowest concentration with no visible turbidity; MBC: Lowest concentration with no colony growth upon subculture. MIC and MBC values for plant extracts are expressed in mg/mL. Different superscript letters within the same column indicate statistically significant differences (Duncan's test, $p < 0.05$).

Development and characterization of chitosan-based hydrogel matrix

Swelling behavior

The percentage swelling of chitosan: PVA hydrogels at varying polymer ratios is presented in **Figure 2(a)**. Overall swelling capacity ranged from approximately 118 to 240% across all formulations and time intervals. At the 1:1 ratio, the highest swelling was observed at all three time points (220 - 238%), with values remaining relatively stable across 30, 60, and 90 min, suggesting rapid water uptake equilibrium. The 1.5:0.5 ratio produced the lowest swelling values (118 - 133%) among all stable formulations. A non-monotonic trend was observed with increasing chitosan proportion: swelling progressively decreased up to the 1.5:0.5 ratio, beyond which it increased again at the 1.75:0.25 ratio, possibly due to the higher hydrophilicity of chitosan's free amino groups at elevated concentrations. The 2:0 formulation (chitosan only, without PVA) exhibited physical disintegration upon immersion and was therefore excluded from further analysis. This observation highlights the essential role of PVA in maintaining structural integrity of the hydrogel network through the formation of intermolecular hydrogen bonds between PVA hydroxyl groups and chitosan amino groups. This trend can be attributed to the competing effects of chitosan and PVA on network structure. PVA contributes extensive hydroxyl groups that facilitate hydrogen bonding with water molecules, thereby enhancing water uptake. As PVA content decreases, the hydrophilic network becomes less expansive and crosslink density increases, reducing swelling capacity [31]. This is consistent with previous reports on chitosan/PVA composite hydrogels, where swelling ratio was shown to be sensitive to polymer composition and the balance between chitosan's rigid polysaccharide backbone and PVA's flexible hydrophilic chains [17]. For dental wound dressing applications, high swelling capacity is desirable as it promotes absorption of wound exudate and maintains a moist healing environment conducive to tissue regeneration [32]. Based on these results, the 1:1 ratio was selected as the optimal formulation for further development, owing to its consistently high swelling capacity, rapid water uptake equilibrium, and low variability across all time points.

FTIR characterization

ATR-FTIR spectra of chitosan/PVA hydrogel without extract (Hydrogel) and extract-loaded hydrogels are presented in **Figure 2(b)**. The hydrogel exhibited characteristic peaks at 3,258 and 3,230 cm^{-1} (O–H and N–H stretching), 2,992 cm^{-1} (C–H stretching), 1,636 cm^{-1} (amide I, C=O stretching), 1,542 cm^{-1} (amide II, N–H bending coupled with C–N stretching), 1,406 cm^{-1} (C–H bending), 1,340 cm^{-1} (C–N stretching), and 1,067 cm^{-1} (C–O–C ether linkage), consistent with previously reported spectra for chitosan/PVA systems [18]. Upon incorporation of plant extracts, the overall spectral profiles remained largely similar to that of the hydrogel, indicating that the fundamental polymer network was preserved. Minor shifts in the O–H/N–H stretching region (3,230 - 3,261 cm^{-1}) and slight wavenumber changes in the amide I band (1,636 to 1,624 - 1,551 cm^{-1}) were observed, suggesting weak non-covalent interactions, primarily hydrogen bonding, between phenolic hydroxyl groups of the extracts and the chitosan/PVA matrix. A slight shift of the C–O–C stretching from 1,067 to 1,028 cm^{-1} and minor peaks around 817 - 923 cm^{-1} were also noted, possibly reflecting aromatic C–H out-of-plane bending of incorporated phenolic compounds. Overall, the FTIR data suggest successful incorporation of plant extracts into the hydrogel matrix through non-covalent interactions, without significant disruption of the polymer backbone structure.

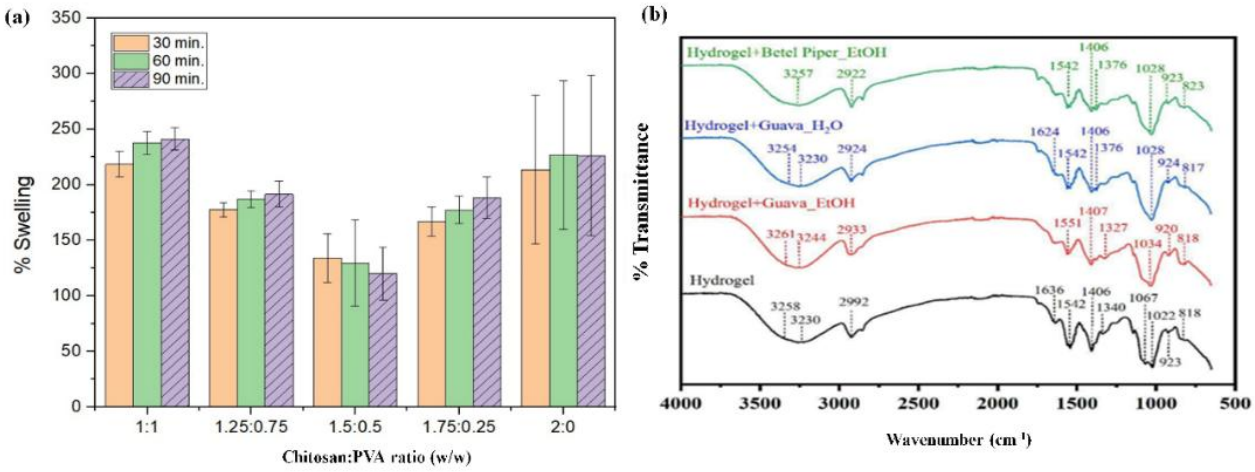


Figure 2 (a) Percentage swelling of chitosan: PVA hydrogel at different ratios (1:1, 1.25:0.75, 1.5:0.5, 1.75:0.25, and 2:0, w/w) measured at 30, 60, and 90 min. (b) ATR-FTIR spectra of chitosan/PVA hydrogel without extract (Hydrogel) and hydrogels incorporated with *Psidium guajava* ethanol extract (Hydrogel+Guava_EtOH), *P. guajava* water extract (Hydrogel+Guava_H_2O), and *Piper betle* ethanol extract (Hydrogel+Betel Piper_EtOH).

Antibacterial activity of extract-loaded chitosan/PVA hydrogels

The antibacterial activity of chitosan/PVA hydrogel and extract-loaded formulations against *S. mutans*, *S. aureus*, and *E. coli* is presented in **Figure 3**. All extract-loaded hydrogels demonstrated significantly enhanced inhibition zones compared to the chitosan/PVA hydrogel across all three bacterial strains ($p < 0.05$), confirming the contribution of incorporated plant bioactive compounds to the overall antibacterial efficacy of the formulations.

The chitosan/PVA hydrogel itself produced measurable inhibition zones against all tested bacteria (7.82 ± 0.04 mm for *S. mutans*, 8.12 ± 0.11 mm for *S. aureus*, and 9.90 ± 0.14 mm for *E. coli*), consistent with the well-established intrinsic antimicrobial mechanism of chitosan [33]. The positively charged amino groups ($–NH_3^+$) of chitosan under acidic to near-neutral pH conditions interact electrostatically with negatively charged components of bacterial cell membranes, increasing membrane permeability, inducing leakage of intracellular contents, and ultimately leading to cell death [34]. This cationic nature of chitosan also facilitates adhesion to negatively charged bacterial surfaces, enhancing its contact-dependent antibacterial action and contributing to biofilm disruption in oral pathogens including *S. mutans* [33,35].

Incorporation of *P. guajava* water extract into the chitosan hydrogel produced the largest inhibition zones across all three bacterial targets, reaching 13.86 ± 0.09 mm against *S. mutans*, 13.58 ± 0.08 mm against *S. aureus*, and 17.44 ± 0.13 mm against *E. coli*. These values represented increases of 77.2%, 67.2%, and 76.2%, respectively, relative to the plain chitosan hydrogel. The superior broad-spectrum activity of this formulation can be attributed to synergistic interactions between chitosan and the diverse phenolic constituents of *P. guajava* water extract. The antibacterial mechanism of quercetin, a principal bioactive constituent well-documented in *P. guajava* leaves, encompasses multiple concurrent pathways including cell membrane damage, increased membrane permeability, inhibition of nucleic acid and protein synthesis, suppression of virulence factor expression, and interference with biofilm formation, all of which can act additively with chitosan's membrane-disrupting mechanism to produce enhanced inhibitory effects [36]. Furthermore, recent metabolomic and transcriptomic studies have demonstrated that quercetin disrupts bacterial fatty acid biosynthesis through direct inhibition of β-ketoacyl-acyl carrier protein reductase (FabG), causing membrane lipid remodeling that compromises structural integrity of the bacterial cell membrane, providing a mechanistic basis for the potent activity

observed particularly against Gram-positive strains such as *S. aureus* [37].

The *P. guajava* ethanol extract-loaded hydrogel showed inhibition zones of 13.42 ± 0.11 mm, 13.44 ± 0.09 mm, and 15.30 ± 0.10 mm against *S. mutans*, *S. aureus*, and *E. coli*, respectively, with no statistically significant differences from the water extract formulation for *S. mutans* and *S. aureus* ($p > 0.05$), while a significant difference was observed for *E. coli* ($p < 0.05$). This difference may reflect variations in the phenolic composition between water and ethanol extracts, as aqueous extraction tends to recover more polar, water-soluble phenolic glycosides that may diffuse more readily through agar under well diffusion conditions, thereby producing larger inhibition zones. The diverse structures of bioactive compounds can complicate the extraction process due to differences in polarity and solubility, which directly influence the type and quantity of compounds recovered by each solvent system [38].

P. betle ethanol extract-loaded hydrogel demonstrated the lowest activity among the three formulations (12.36 ± 0.05, 13.04 ± 0.11, and 13.72 ± 0.13 mm against *S. mutans*, *S. aureus*, and *E. coli*, respectively), yet remained significantly greater than the plain hydrogel across all organisms ($p < 0.05$). The relatively lower activity compared to *P. guajava*-loaded hydrogels may reflect the lower polarity and aqueous solubility and diffusibility of hydroxychavicol, a hydrophobic phenolic compound predominant in *P. betle* extract, compared to the more polar, water-soluble phenolic glycosides of *P. guajava* [35]. The combination of phenolic-mediated cell wall disruption with chitosan's electrostatic membrane mechanism represents a dual-target approach that may reduce the likelihood of resistance development compared to single-target agents [34].

Notably, inhibition zones against *E. coli* were consistently larger than those against *S. mutans* and *S. aureus* across all hydrogel formulations, contrasting with the pattern observed for crude extracts alone. This may be attributed to chitosan's ability to chelate divalent cations (Mg^{2+} and Ca^{2+}) that stabilize the lipopolysaccharide layer of Gram-negative outer membranes, thereby facilitating phenolic compound penetration and broadening the antimicrobial spectrum of the composite system [39]. Although all formulations showed lower activity than chlorhexidine (25.8 ± 0.40 mm against *S. mutans*), the extract-loaded hydrogels demonstrated meaningful antibacterial activity against all tested oral pathogens, supporting their potential as natural antimicrobial biomaterial candidates for post-dental extraction applications. All three formulations were therefore selected for further release profile investigation.

Phenolic compound release profiles and antioxidant activity of hydrogel formulations

The release profiles of TPC and corresponding DPPH radical scavenging activity from extract-loaded chitosan hydrogels at 6 and 24 h are presented in **Figure 4**. Distinct release patterns were observed among the three formulations, reflecting differences in the physicochemical nature of the incorporated extracts and their interactions with the chitosan/PVA polymer matrix. The *P. guajava* water extract-loaded hydrogel (gel@gua Water) exhibited the highest TPC release at 6 h (2.38 mg GAE/mL), which decreased substantially by 24 h (0.30 mg GAE/mL). This pattern of rapid early release followed by a decline at 24 h suggests preferential release of polar phenolic compounds present in the water extract, particularly gallic acid, quinic acid, and catechin glycosides, which diffuse readily through the hydrophilic hydrogel matrix upon initial contact with the release medium [40]. In polyphenol-based hydrogel systems, phenolic compounds interact with the chitosan/PVA polymer matrix primarily through hydrogen bonding between hydroxyl groups and the polymer backbone, as well as π–π stacking interactions among aromatic rings. The compounds with lower molecular weight and higher polarity tend to be released rapidly during initial swelling, while those forming stronger non-covalent interactions with the matrix are retained longer [41]. The high TPC release at 6 h was accompanied by a correspondingly high DPPH inhibition (~65%), confirming that the released phenolics retained significant antioxidant functionality. This is particularly relevant in the context of post-extraction wound healing, where reactive oxygen species generated during the inflammatory phase have been reported to impair tissue regeneration [42].

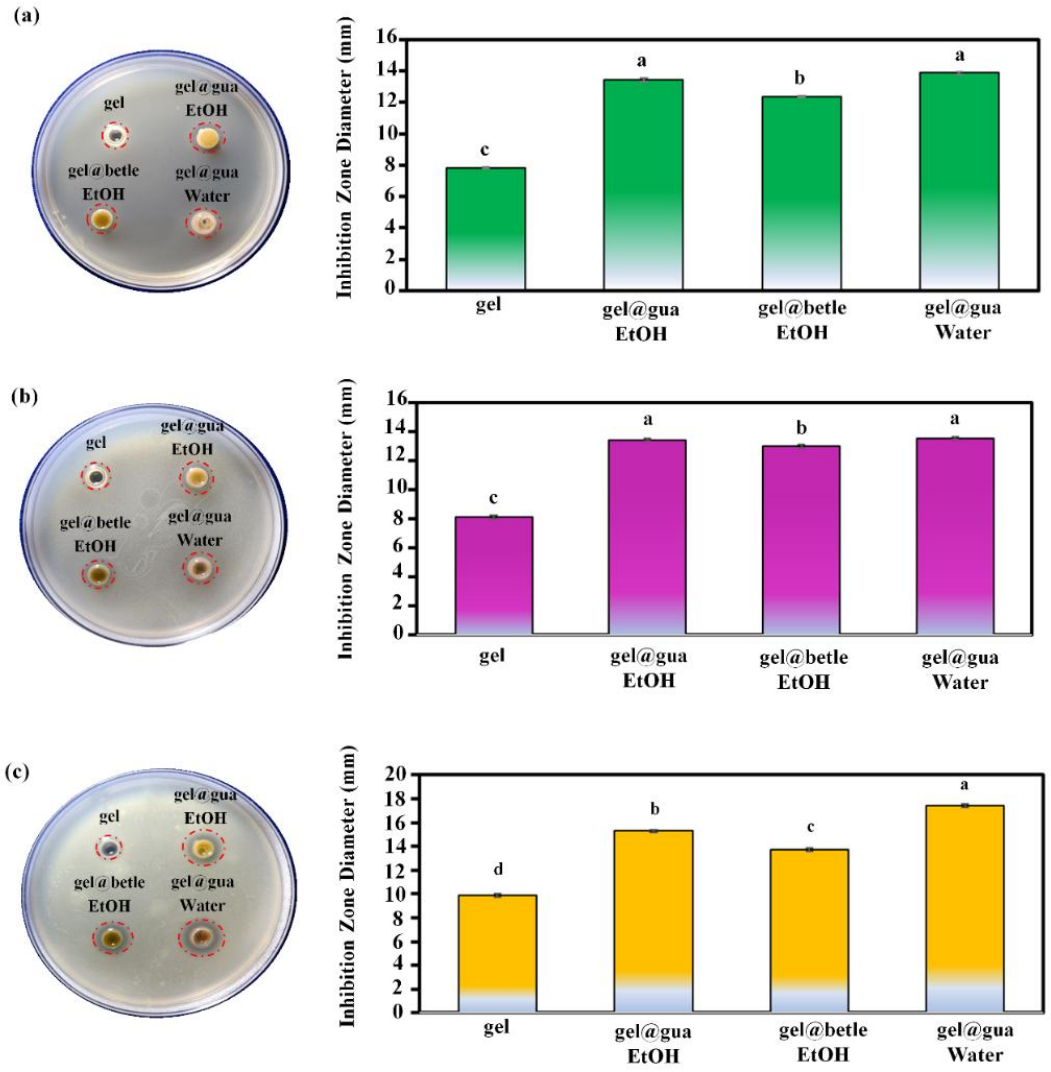


Figure 3 Antibacterial activity of chitosan/PVA hydrogel (gel), gel@gua EtOH, gel@betle EtOH, and gel@gua Water against (a) *Streptococcus mutans*, (b) *Staphylococcus aureus*, and (c) *Escherichia coli* determined by agar well diffusion method. Data are expressed as mean ± SD. Different letters indicate statistically significant differences among formulations (Duncan's test, $p < 0.05$).

In contrast, the *P. betle* ethanol extract-loaded hydrogel (gel@betle EtOH) demonstrated minimal TPC release at 6 h (~0.4 mg GAE/mL) but showed a substantial increase at 24 h (~1.6 mg GAE/mL), alongside a corresponding rise in DPPH inhibition (~70%). This pattern of gradual phenolic release over 24 h may be consistent with a diffusion-mediated process, as has been reported for hydrophobic compounds released from chitosan-based hydrogel systems [41], though formal kinetic modeling with additional time points would be required to confirm the release mechanism in the present formulation. The prolonged release profile of the *P. betle* formulation may therefore be advantageous for applications requiring prolonged antioxidant protection over 24 h or more, such as post-extraction socket management where healing extends across multiple days.

The *P. guajava* ethanol extract-loaded hydrogel showed an intermediate profile, with moderate TPC release at 6 h (~0.4 mg GAE/mL) with a slight decline at 24 h (~0.3 mg GAE/mL), with corresponding DPPH inhibition values of approximately 60% and 55%, respectively. The lower release compared to the water extract formulation despite similar polymer composition suggests that the relatively less polar character of the ethanol extract components results in stronger entrapment within the hydrophobic domains of the polymer network.

Chitosan/PVA hydrogel showed minimal TPC release at both time points (~0.05 - 0.1 mg GAE/mL), confirming that the phenolic signal is derived entirely from the incorporated plant extracts rather than the polymer matrix itself. The combination of polyphenols with hydrogel matrices not only enhances the stability of labile phenolic compounds against oxidation and degradation but also enables controlled spatiotemporal delivery of bioactives to the wound site, providing synergistic therapeutic effects that neither the polymer nor the polyphenols could achieve independently [43].

Collectively, the two distinct release profiles identified here represent complementary therapeutic strategies for post-dental extraction wound management. The rapid early release observed in the *P. guajava* water extract formulation and the prolonged release over 24 h of the *P. betle* ethanol extract formulation offer different but mutually supportive approaches to delivering antioxidant phenolics across the wound healing timeline. The rapid early release profile may be particularly suited to immediate post-extraction care, providing a high initial dose of antioxidant phenolics during the acute inflammatory phase, while the prolonged release profile of the *P. betle* formulation may offer continued antioxidant coverage during the subsequent proliferative phase, a premise that warrants further biological investigation. These findings suggest that a combination or sequential use of these two formulations could offer temporal coverage across multiple phases of wound healing, a strategy warranting further investigation.

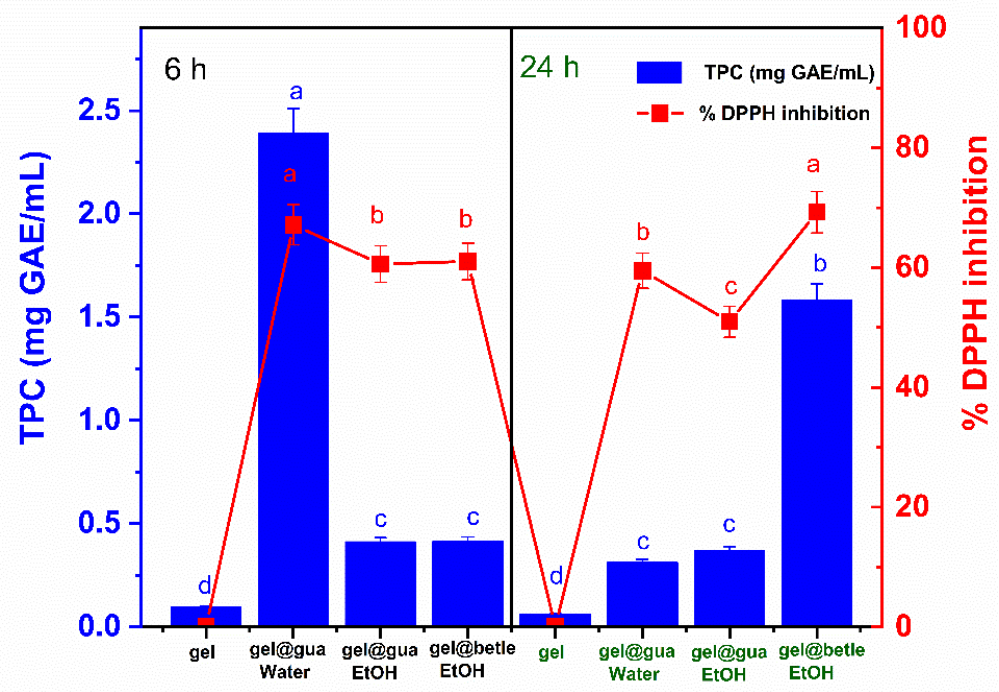


Figure 4 Total phenolic content (TPC, mg GAE/mL) and DPPH radical scavenging activity (%) of compounds released from chitosan/PVA hydrogel and extract-loaded formulations into PBS (pH 6.8, 37 °C, 50 rpm) at 6 h and 24 h. Different lowercase letters indicate statistically significant differences among formulations at the same time point (Duncan's test, $p < 0.05$).

Chemical composition analysis and molecular docking with COX-2

Given the superior antibacterial activity and favorable release profile demonstrated by the *P. guajava* aqueous extract-loaded hydrogel, this formulation was selected for further chemical characterization. LC-MS/MS analysis was subsequently performed to identify the principal bioactive phenolic constituents responsible for the observed biological activities, providing a mechanistic basis for the antibacterial and antioxidant properties. LC-MS/MS profiling of *P. guajava* extract in negative ionization mode annotated 24 compounds at varying confidence levels (**Table 3**). Compounds with library match scores of ≥ 80 were

tentatively identified based on accurate mass, MS/MS fragmentation patterns, and Metlin library matching, while those with scores below 80 or with no available library match (score = 0) were putatively annotated. The tentatively identified compounds (library score ≥ 80) span phenolic acids (gallic acid, quinic acid), flavan-3-ols (catechin, epigallocatechin, procyanidin B2), a flavone glycoside (hieracin), flavonols (quercetin, myricetin) and a flavonol glycoside (quercetin 3-galactoside), a dihydrochalcone (phloridzin), a stilbenoid glycoside (rhapontin), and triterpenoids (maslinic acid). In addition, several putatively annotated compounds were assigned to flavonol glycosides (myricetin 3-arabinoside, kaempferol 4'-glucoside), a stilbenoid glycoside (piceatannol 4'-galloylglucoside), an ellagitannin (guavin B), a benzophenone derivative (maclurin derivative), triterpenoids (bayogenin, betulinic acid), and other tentative structures (3-trans-p-coumaroylrotundic acid, cis-p-coumaroylcorosolic acid, Macrourone C), pending confirmation with authentic standards. A non-phenolic disaccharide, sucrose, was also detected.

In terms of relative abundance, the putatively annotated compound Macrourone C was the dominant feature (19.60%), followed by the putatively annotated Tricetin 3'-xyloside (13.96%) and Piceatannol 4'-galloylglucoside (8.08%), the tentatively identified Sucrose (7.92%), the putatively annotated Kaempferol 4'-glucoside (7.64%) and the tentatively identified Quercetin 3-galactoside (7.45%) (**Table 3**). Macrourone C, the most abundant putatively annotated compound, was assigned based solely on accurate mass (score = 0) without corroborating MS/MS evidence. This compound class has been previously reported as a Diels–Alder type adduct from *Morus macroura* (Moraceae) [44], a species taxonomically distinct from *P. guajava*, and requires further structural confirmation with authentic standards. Among the tentatively identified bioactive phenolics, quercetin (2.71%) and myricetin (0.20%) were present at lower relative abundances but hold particular pharmacological significance. Although several compounds with higher relative abundance were detected, a number of these lacked library match scores (score = 0) and were annotated as putative identifications based solely on accurate mass data, precluding confident structural assignment. Quercetin has been shown to downregulate key inflammatory mediators including iNOS, COX-2, NF-κB, and C-reactive protein in human hepatocyte-derived cells [45]. Myricetin has been reported to act as a naturally occurring co-substrate of cyclooxygenases, modulating prostaglandin biosynthesis in a dose-dependent biphasic manner, with stimulatory effects at low doses and inhibitory effects at higher doses, suggesting concentration-dependent regulatory interactions with COX enzymes [46]. These two flavonoids were therefore selected for molecular docking analysis against COX-2 to computationally explore potential anti-inflammatory interactions as a basis for future experimental investigation.

Table 3 Compounds identified in water extract of *P. guajava* leaves using liquid chromatography-tandem mass spectrometry (LC-MS/MS) analysis in negative ionization mode.

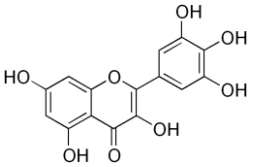
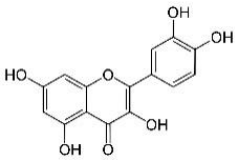
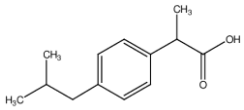
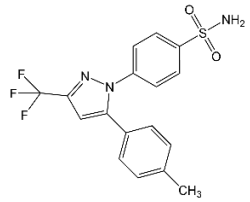
Peak no.	Compound name	Retention time (min)	Observed mass (m/z)	Mass (g/mol)	Score (Lib)	Relative abundance (%)
1	Quinic acid	1.484	191.0562	192.0635	92.33	1.57
2	Sucrose	1.559	341.1092	342.1165	98.08	7.92
3	Gallic acid	4.239	169.0141	170.0213	90.21	0.24
4	Epigallocatechin	6.094	305.0668	306.0741	96.35	0.74
5	Procyanidin B2	7.810	577.1353	578.1424	84.39	0.77
6	(±)-Catechin	8.612	289.0717	290.0790	93.62	2.91
7	Myricetin 3-arabinoside	12.733	449.0726	450.0799	0	1.66
8	Hieracin	13.058	301.0354	302.0426	96.49	0.45

Peak no.	Compound name	Retention time (min)	Observed mass (m/z)	Mass (g/mol)	Score (Lib)	Relative abundance (%)
9	Quercetin 3-galactoside	13.209	463.0884	464.0957	96.43	7.45
10	Maclurin 3-C-(6"-p-hydroxybenzoyl-glucoside)	14.336	543.1145	544.1218	0	4.47
11	Tricetin 3'-xyloside	14.512	433.0785	434.0857	0	13.96
12	Kaempferol 4'-glucoside	14.725	447.0937	448.1009	0	7.64
13	Myricetin	15.363	317.0305	318.0378	85.39	0.2
14	Phloridzin	15.902	435.1299	436.1371	99.00	0.4
15	Rhapontin	16.567	419.1347	420.1420	84.61	1.89
16	Guavin B	18.307	693.1092	694.1165	0	0.35
17	Piceatannol 4'-galloylglucoside	18.320	557.1301	558.1373	0	8.08
18	Quercetin	18.533	301.0354	302.0427	98.54	2.71
19	Bayogenin	28.643	487.3428	488.3501	0	1.42
20	3-trans-p-Coumaroylrotundic acid	35.859	633.3794	634.3867	0	4.27
21	Maslinic Acid	37.262	471.3478	472.3551	88.69	2.77
22	cis-p-Coumaroylcorosolic acid	42.974	617.3847	618.3919	0	7.70
23	Macrourone C	43.375	491.2449	492.2519	0	19.60
24	Betulinic Acid	44.465	455.3531	456.3603	64.48	0.83

Note: Mass (g/mol) represents the neutral monoisotopic mass of each compound. Observed mass (m/z) corresponds to the deprotonated ion $[M-H]^-$ detected in negative ionization mode. Score (Lib) indicates the library match score obtained from the Metlin database; a score of 0 indicates no available library match; such compounds were putatively annotated based on accurate mass data only and require confirmation with authentic reference standards. Relative abundance (%) was calculated as the percentage of each compound's peak height relative to the total peak height of all 24 identified compounds.

Prior to screening of the test compounds, the docking protocol was validated by redocking ibuprofen into the COX-2 active site (PDB ID: 4PH9), successfully reproducing its known binding interactions with key active site residues including TYR356 and ARG121, with an RMSD of 1.07 Å relative to the original X-ray crystallographic conformation, consistent with the accepted validation threshold of ≤ 2.0 Å. Docking results presented in **Table 4** and **Figure 5** show that both flavonoids exhibit favorable predicted binding affinity toward COX-2 relative to the reference NSAID ibuprofen, though not exceeding that of the selective COX-2 inhibitor celecoxib. Myricetin achieved the most favorable binding energy among the test flavonoids (-8.68 kcal/mol, % DS = 100), followed by quercetin (-8.59 kcal/mol, % DS = 92), both substantially outperforming ibuprofen (-6.77 kcal/mol, % DS = 85). Celecoxib, included as a selective COX-2 inhibitor reference, exhibited the highest predicted binding affinity of all compounds tested (-11.11 kcal/mol, % DS = 100), providing a comparative benchmark for selective COX-2 inhibitory interactions. These results suggest that while myricetin and quercetin demonstrate stronger predicted binding than a non-selective NSAID, their predicted affinities remain below that of a dedicated selective COX-2 inhibitor, consistent with their status as naturally occurring polyphenols rather than optimized pharmacological agents.

Table 4 Chemical identification of key bioactive compounds in *P. guajava* extract and their molecular interactions with COX-2.

Compounds	Structure	Molecular docking with COX-2	
		Binding energy (kcal/mol)	% DS
Myricetin		-8.68	100
Quercetin		-8.59	92
*Ibuprofen		-6.77	85
*Celecoxib		-11.11	100

Note: Molecular docking was performed against cyclooxygenase-2 (COX-2) using AutoDock 4.2. Binding energy (kcal/mol) represents the predicted binding free energy; more negative values indicate stronger predicted binding affinity. % DS represents the percentage of docking solutions within the most populated cluster from 100 independent runs. *Ibuprofen and celecoxib were included as referent ligands representing a non-selective NSAID and a selective COX-2 inhibitor, respectively, for comparative binding affinity assessment.

Analysis of key binding interactions revealed distinct residue engagement for each compound. Celecoxib (**Figure 5(a)**) interacted with PHE519 through hydrogen bonding, consistent with its known binding within the secondary hydrophobic pocket of COX-2 that confers selectivity over COX-1. Ibuprofen (**Figure 5(b)**) formed hydrogen bonds primarily with TYR356 and ARG121, consistent with classical NSAID binding at the carboxylate channel entrance. Myricetin (**Figure 5(c)**) interacted with MET523, GLN193, SER354, and HIS90 through multiple hydrogen bonds facilitated by its additional 5'-hydroxyl group on the B-ring, which is absent in quercetin. This trihydroxylated B-ring of myricetin enables formation of more extensive hydrogen bonds within the COX-2 active site compared to the dihydroxylated catechol B-ring of quercetin, explaining its marginally superior binding energy. Quercetin (**Figure 5(d)**) engaged SER530, SER354, TYR356, and GLN193, with SER530 being the catalytic serine residue whose acetylation by aspirin underpins irreversible COX inhibition [47], suggesting a putative mechanistic overlap between quercetin and established NSAIDs through competitive occupancy of this critical site.

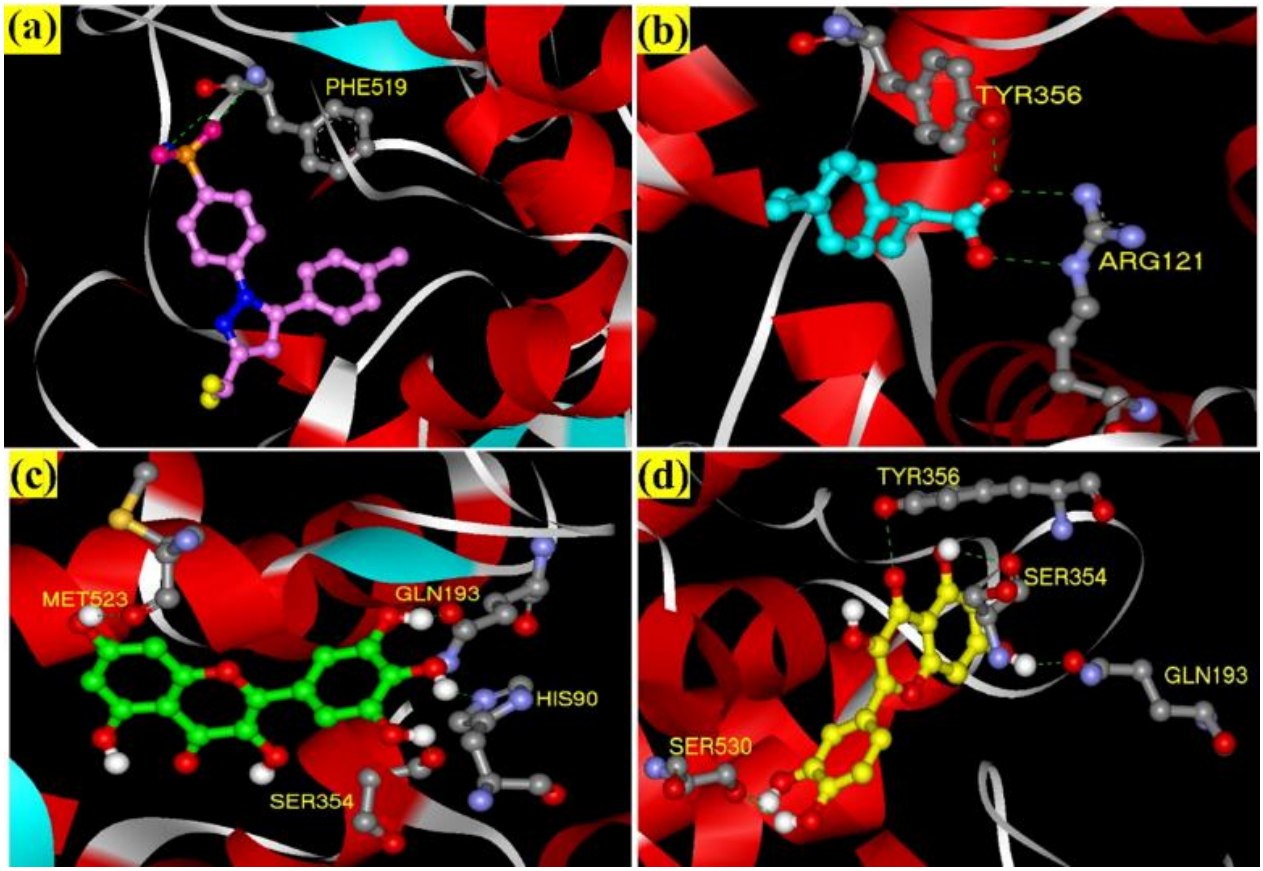


Figure 5 Molecular docking of ligands within the COX-2 active site. (a–d) Key hydrogen bond interactions (dashed green lines) of celecoxib, ibuprofen (IBP), myricetin, and quercetin with COX-2 active site residues, respectively.

These computational findings are consistent with the experimental results obtained in preceding sections. LC-MS/MS confirmed the presence of quercetin and myricetin in the *P. guajava* water extract, alongside their glycoside derivatives. The release profile data demonstrated that phenolic compounds from the *P. guajava* water extract-loaded hydrogel are released within 6 h with retention of significant antioxidant activity, coinciding with the acute inflammatory phase of post-extraction wound healing during which COX-2 activity is most pronounced. Collectively, the findings of this study suggest a multi-mechanistic framework of potential therapeutic action encompassing three complementary levels of activity. At the microbial level, the broad-spectrum antibacterial activity arises from synergistic interactions between chitosan's electrostatic disruption of bacterial cell membranes and the multi-target antimicrobial activity of phenolic compounds. At the oxidative level, the high TPC and rapid phenolic release profile provide immediate antioxidant protection during the inflammatory phase. At the molecular level, preliminary docking analysis predicted favorable binding interactions of myricetin and quercetin at the COX-2 active site, with computed binding energies exceeding that of ibuprofen, providing a computational basis for potential anti-inflammatory activity that warrants further experimental validation. To the best of our knowledge, this study represents the first comprehensive *in vitro* characterization of *P. guajava* and *P. betle* extract-loaded chitosan/PVA hydrogels for dental wound management applications.

Study limitations and future perspectives

Despite the encouraging *in vitro* results obtained in this study, several limitations must be considered when interpreting the findings and planning subsequent research toward dental wound care applications. Biocompatibility of the composite hydrogel formulations was not assessed in the current work. Although chitosan, PVA, and the plant extracts used

here are individually regarded as low-toxicity materials in the existing literature, cytotoxicity testing using relevant oral cell models such as human oral keratinocytes or gingival fibroblasts will be an important next step before translational conclusions can be drawn. Additional biological characterization, including antibiofilm activity, hemocompatibility, mucoadhesion, and cell-based anti-inflammatory assays, falls outside the scope of this initial study and is recommended for subsequent investigations.

The COX-2 inhibitory potential suggested by molecular docking represents a hypothesis to be explored experimentally rather than a definitive mechanistic finding. Although the docking protocol was validated through redocking of the co-crystallized ligand ibuprofen, and celecoxib was included as a selective COX-2 inhibitor reference for comparative binding affinity assessment, molecular dynamics simulation to assess binding stability under physiological conditions is recommended for future computational studies to further strengthen the reliability of the predicted interactions.

From a formulation perspective, rheological characterization and degradation profiling under simulated oral conditions would further define the practical performance of these hydrogels as intraoral wound dressings and are planned for future work. Finally, *in vivo* validation using an appropriate animal model remains a necessary step toward preclinical development. Future studies may also explore sequential or combined application of the rapid early-release and prolonged-release formulations developed here, with the aim of providing coordinated therapeutic coverage across multiple phases of dental wound healing.

Conclusions

This study provides *in vitro* evidence that chitosan/PVA hydrogels incorporating *Psidium guajava* and *Piper betle* extracts can function as multifunctional biomaterial candidates with complementary antimicrobial and antioxidant actions relevant to post-dental extraction wound management. The two distinct phenolic release profiles suggest that these systems may address different phases of the wound healing timeline within a single material class, with the rapid early release from the *P. guajava* water extract formulation potentially suited to the acute inflammatory phase and the prolonged release over 24 h from the *P. betle* ethanol extract formulation offering continued antioxidant coverage during the subsequent proliferative phase. Molecular docking further provided a computational basis for potential COX-2 inhibitory activity of the identified flavonoids, supporting a multi-mechanistic framework of potential therapeutic action that warrants experimental validation. These findings provide a preliminary scientific basis for advancing *P. guajava* and *P. betle* extract-loaded chitosan/PVA hydrogels toward further preclinical evaluation as plant-derived biomaterials for dental wound care.

CRediT Author Statement

Parichat Thepthong: Methodology; Validation; Formal analysis; Supervision; Writing – review & editing. **Panita Kongsune**: Conceptualization; Methodology; Formal analysis; Supervision; Writing – review & editing. **Patcharakorn Raksasee**: Investigation; Data curation; Visualization; Writing – original draft. **Safira Minham**: Investigation; Data curation; Visualization; Writing – original draft. **Netnapa Chana**: Conceptualization; Methodology; Resources; Funding acquisition; Supervision; Project administration; Writing – review & editing.

Declaration of generative AI in scientific writing

Claude (Anthropic) was employed to enhance the linguistic quality and readability of this manuscript under continuous human oversight. The AI tool was not involved in research methodology, data generation, or scientific interpretation. All intellectual content and conclusions remain solely the responsibility of the authors.

References

[1] G Lodi, L Azzi, EM Varoni, M Pentenero, MD Fabbro, A Carrassi, A Sardella and M Manfredi. Antibiotics to prevent complications following tooth extractions. *Cochrane Database of Systematic Reviews* 2021; **2**, CD003811.

[2] P Dignam, M Elshafey, A Jeganathan, M Foo, JS Park and M Ratnaweera. Prevalence and factors influencing post-operative complications following tooth extraction: A narrative review.

International Journal of Dentistry 2024; **2024**, 7712829.

[3] MD Rossary, JKP Djunaedi, TPR Riyantoro and A Setiawati. Tailoring strategy of chitosan-based hydrogel for improving wound healing: A systematic review. *Trends in Sciences* 2025; **22(11)**, 11023.

[4] X Zhou, C Liu, Y Han, C Li, S Liu, X Li, G Zhao and Y Jiang. An antibacterial chitosan-based hydrogel as a potential degradable bio-scaffold for alveolar ridge preservation. *RSC Advances* 2022; **12(50)**, 32219-32229.

[5] H Chen, M Hu, N Liu and Y Li. Research progress on modified chitosan hydrogels for tissue repair and regeneration. *Carbohydrate Polymers* 2026; **385**, 125347.

[6] Z Zeng, L Kang, Y He, Y Guan, Y Cao, X Zhang and WE Yuan. A chitosan-tea polyphenol composite hydrogel with integrated antibacterial, antioxidant and immunomodulatory functions for the tissue regeneration of MRSA-infected wounds. *Bioorganic Chemistry* 2026; **174**, 109722.

[7] A Sirinthipaporn and W Jiraungkoorskul. Wound healing property review of Siam weed, *Chromolaena odorata*. *Pharmacognosy Reviews* 2017; **11(21)**, 35-38.

[8] J Seo, U Lee, S Seo, AE Wibowo, OB Pongtuluran, K Lee, SB Han and S Cho. Anti-inflammatory and antioxidant activities of methanol extract of *Piper betle* L. leaves and stems by inhibiting NF-κB/MAPK/Nrf2 signaling pathways in RAW 264.7 macrophages. *Biomedicine & Pharmacotherapy* 2022; **155**, 113734.

[9] Y Andriana, TD Xuan, TN Quy, TN Minh, TM Van and TD Viet. Antihyperuricemia, antioxidant, and antibacterial activities of *Tridax procumbens* L. *Foods* 2019; **8(1)**, 21.

[10] HD Huynh, P Nargotra, HMD Wang, CJ Shieh, YC Liu and CH Kuo. Bioactive compounds from guava leaves (*Psidium guajava* L.): Characterization, biological activity, synergistic effects, and technological applications. *Molecules* 2025; **30(6)**, 1278.

[11] S Bhagavathy, C Mahendiran and R Kanchana. Identification of glucosyl transferase inhibitors from *Psidium guajava* against *Streptococcus mutans* in dental caries. *Journal of Traditional and Complementary Medicine* 2019; **9(2)**, 124-137.

[12] A Sakthivel, K Sankaran, G Rengasamy, VV Priya and P Sathishkumar. Formulation of mouthwash using combined herbal extracts to control the predominant oral pathogens and biofilm. *Journal of Herbal Medicine* 2024; **46**, 100905.

[13] NNT Nguyen, TTD Nguyen, TS Nguyen, DTM Than, TTY Le and HN Nguyen. Nanoemulsion-based mouthwash with *Litsea cubeba* essential oil and *Piper betle* extract for inflammatory dental condition. *Pharmacia* 2025; **72**, 1-17.

[14] R Teanpaisan, P Kawsud, N Pahumunto and J Puripattanavong. Screening for antibacterial and antibiofilm activity in Thai medicinal plant extracts against oral microorganisms. *Journal of Traditional and Complementary Medicine* 2017; **7(2)**, 172-177.

[15] C Lorena, A Ressaissi and ML Serralheiro. Bioactives from *Psidium guajava* leaf decoction: LC-HRMS-MS-Qtof identification, bioactivities and bioavailability evaluation. *Food Chemistry Advances* 2022; **1**, 100003.

[16] WX Waresindo, HR Luthfianti, D Edikresnha, T Suciati, FA Noor and K Khairurrijal. A freeze–thaw PVA hydrogel loaded with guava leaf extract: Physical and antibacterial properties. *RSC Advances* 2021; **11(48)**, 30156-30171.

[17] ER Kenawy, EA Kamoun, SM Elsigeny, S Heikal, AA El-Shehawy and YAG Mahmoud. Vanillin loaded-physically crosslinked PVA/chitosan/itaconic membranes for topical wound healing applications. *Journal of Applied Biomaterials & Functional Materials* 2024. https://doi.org/10.1177/22808000241281273

[18] DM Suflet, I Popescu, IM Pelin, DL Ichim, OM Daraba, M Constantin and G Fundueanu. Dual cross-linked chitosan/PVA hydrogels containing silver nanoparticles with antimicrobial properties. *Pharmaceutics* 2021; **13(9)**, 1461.

[19] P Kongsune, K Sangthongchin, P Ampha, M Maneechote and N Chana. Enhancement of antioxidant activity and inhibition of polyphenol oxidase from green oak lettuce by chitosan-encapsulated rambutan (*Nephelium lappaceum* L.) peel extract. *Chiang Mai Journal of Science* 2025; **52(4)**, e2025035.

[20] BJ Orlando, MJ Lucido and MG Malkowski. The structure of ibuprofen bound to cyclooxygenase-2. *Journal of Structural Biology* 2015; **189(1)**, 62-66.

[21] QD Do, AE Angkawijaya, PL Tran-Nguyen, LH Huynh, FE Soetaredjo, S Ismadji and YH Ju. Effect of extraction solvent on total phenol content, total flavonoid content, and antioxidant activity of *Limnophila aromatica*. *Journal of Food and Drug Analysis* 2014; **22(3)**, 296-302.

[22] T Singh, VK Pandey, SA Mukarram, R Singh, KK Dash and B Kovács. Ultrasound assisted extraction of phytochemicals from *Piper betle* L. *Ultrasonics Sonochemistry* 2024; **106**, 106894.

[23] ND Anh, CN Linh, LTM Hiep and DV Kien. Application of *Piper betle* leaf extract as a bioactive additive in eco-friendly antifouling coatings. *Surfaces* 2025; **8(4)**, 72.

[24] KMSAK Dehideniya, VP Bulugahapitiya, RS Sabaragamuwa and TC Kananke. Anti-diabetic, lipid peroxidase, antimicrobial, anti-oxidant, general toxicity properties and polyphenol content of *Psidium guajava*, *Garcinia quaesita*, and *Cinnamon verum* extracts along with their potential as nutraceuticals. *Food and Humanity* 2025; **4**, 100537.

[25] J Seo, S Lee, ML Elam, SA Johnson, J Kang and BH Arjmandi. Study to find the best extraction solvent for use with guava leaves (*Psidium guajava* L.) for high antioxidant efficacy. *Food Science & Nutrition* 2014; **2(2)**, 174-180.

[26] EA Ainsworth and KM Gillespie. Estimation of total phenolic content and other oxidation substrates in plant tissues using Folin–Ciocalteu reagent. *Nature Protocols* 2007; **2(4)**, 875-877.

[27] L Ruiz-Vasquez, LR Mesia, MM Maco, JA Zapata, HR Cotrina, M Cobos, V Pinedo-Cancino, F Tello and JC Castro. Optimized Folin–ciocalteu method for determination of total polyphenols in medicinal plants of the Peruvian Amazon: Validation and application to twelve species. *AppliedChem* 2026; **6(1)**, 17.

[28] R Albani, SR Habib, A AlQahtani, AA AlHelal and M Alrabiah. *Streptococcus mutans* and *Porphyromonas gingivalis* adhesion to glazed/polished surfaces of CAD/CAM restorations. *Heliyon* 2024; **10(22)**, e40276.

[29] AM Hall, S Baskiyar, KL Heck, MD Hayden, C Ren, C Nguyen, CD Seals, E Monu and AI Calderón. Investigation of the chemical composition of antibacterial *Psidium guajava* extract and partitions against foodborne pathogens. *Food Chemistry* 2023; **403**, 134400.

[30] D Kurnia, GS Hutabarat, D Windaryanti, T Herlina, Y Herdiyati and MH Satari. Potential allylpyrocatechol derivatives as antibacterial agent against oral pathogen of *S. sanguinis* ATCC 10,556 and as inhibitor of MurA enzymes: *In vitro* and *in silico* study. *Drug Design, Development and Therapy* 2020; **14**, 2977-2985.

[31] S Gupta, TJ Webster and A Sinha. Evolution of PVA gels prepared without crosslinking agents as a cell adhesive surface. *Journal of Materials Science: Materials in Medicine* 2011; **22**, 1763-1772.

[32] M Demeter, A Scărișoreanu and I Călina. State of the art of hydrogel wound dressings developed by ionizing radiation. *Gels* 2023; **9(1)**, 55.

[33] M Nasaj, M Chehelgerdi, B Asghari, A Ahmadieh-Yazdi, M Asgari, S Kabiri-Samani, E Sharifi and M Arabestani. Factors influencing the antimicrobial mechanism of chitosan action and its derivatives: A review. *International Journal of Biological Macromolecules* 2024; **277(P2)**, 134321.

[34] KS Dhlamini, CT Selepe, B Ramalapa, L Tshweu and SS Ray. Reimagining chitosan-based antimicrobial biomaterials to mitigate antibiotic resistance and alleviate antibiotic overuse: A review. *Macromolecular Materials and Engineering* 2024; **309**, 2400018.

[35] EM Costa, S Silva, FK Tavaria and MM Pintado. Study of the effects of chitosan upon *Streptococcus mutans* adherence and biofilm formation. *Anaerobe* 2013; **20**, 27-31.

[36] TLA Nguyen and D Bhattacharya. Antimicrobial activity of quercetin: An approach to its mechanistic principle. *Molecules* 2022; **27(8)**, 2494.

[37] H Yuan, H Xun, J Wang, J Wang, X Yao and F Tang. Integrated metabolomic and transcriptomic analysis reveals the underlying antibacterial mechanisms of the phytonutrient quercetin-induced fatty acids alteration in *Staphylococcus*

aureus ATCC 27217. *Molecules* 2024; **29(10)**, 2266.

[38] K Ratchasong, P Saengsawang, G Yusakul, K Kabploy, HK Lakhanapuram, A Harudeen, P Wintachai, T Thomrongsuwannakij, OF Nwabor and W Mitsuwan. Deep eutectic solvent-based emulsion containing *Piper betle* L. extract and hydroxychavicol prevent biofilm development and surface adhesion of avian pathogenic *Escherichia coli* on stored chicken meat. *Antibiotics* 2026; **15(4)**, 328.

[39] A El-Araby, W Janati, R Ullah, S Ercisli and F Errachidi. Chitosan, chitosan derivatives, and chitosan-based nanocomposites: Eco-friendly materials for advanced applications (a review). *Frontiers in Chemistry* 2024; **11**, 1327426.

[40] G Ekanayake, S Wijayawardana, M Jayanetti, C Thambiliyagodage, H Liyanaarachchi and A Mendis. *In vitro* release kinetics of bioactive compounds (gallic acid, ellagic acid, and eugenol) from chitosan polymer and the bioactivity of herb-loaded chitosan–CuO nanocomposites. *Scientific Reports* 2025; **15(1)**, 35743.

[41] E Morales, M Quilaqueo, R Morales-Medina, S Drusch, R Navia, A Montillet, M Rubilar, D Poncelet, F Galvez-Jiron and A Acevedo. Pectin–chitosan hydrogel beads for delivery of functional food ingredients. *Foods* 2024; **13(18)**, 2885.

[42] K Ukaegbu, E Allen and KKH Svoboda. Reactive oxygen species and antioxidants in wound healing: Mechanisms and therapeutic potential. *International Wound Journal* 2025; **22(5)**, e70330.

[43] R Wang, Z Wang and N Jiang. The preparation, properties, and applications of polyphenol hydrogels for the treatment of oral diseases: A comprehensive overview. *International Journal of Biological Macromolecules* 2025; **321(P3)**, 146310.

[44] PP Putra, A Asnawi, F Hamdayuni, Arfan and LO Aman. Pharmacoinformatics analysis of *Morus macroura* for drug discovery and development. *International Journal of Applied Pharmaceutics* 2024; **16(1)**, 111-117.

[45] V García-Mediavilla, I Crespo, PS Collado, A Esteller, S Sánchez-Campos, MJ Tuñón and J González-Gallego. The anti-inflammatory flavones quercetin and kaempferol cause inhibition of inducible nitric oxide synthase, cyclooxygenase-2 and reactive C-protein, and down-regulation of the nuclear factor kappaB pathway in Chang Liver cells. *European Journal of Pharmacology* 2007; **557(2-3)**, 221-229.

[46] HW Bai and BT Zhu. Myricetin and quercetin are naturally occurring co-substrates of cyclooxygenases *in vivo*. *Prostaglandins Leukotrienes Essent Fatty Acids* 2010; **82(1)**, 45-50.

[47] J Lei, Y Zhou, D Xie and Y Zhang. Mechanistic insights into a classic wonder drug—Aspirin. *Journal of the American Chemical Society* 2015; **137(1)**, 70-73.